APPENDIX

The heptad repeat domain 1 of Mitofusin has membrane destabilization function in mitochondrial fusion

Frédéric Daste, Cécile Sauvanet, Andrej Bavdek, James Baye, Fabienne Pierre, Rémi Le Borgne, Claudine David, Manuel Rojo, Patrick Fuchs, David Tareste

TABLE OF CONTENTS

Supplementary Text

Surface density of HR1 required for liposome fusion vs. physiological concentration of fusion proteins

Our titration experiments revealed that HR1-mediated liposome fusion required a minimal surface density of 1 HR1 protein for 470 lipids (Fig. S5B). How does this density compare with known surface densities of fusion proteins, such as SNARE and Atlastin proteins, as well as with the physiological concentration of Mitofusins in the outer mitochondrial membrane? The concentration of the v-SNARE protein VAMP2 in synaptic vesicles was shown to be about 12,600 molecules/μm^2 [1], whereas the average concentration of the t-SNARE protein Syntaxin 1 at the plasma membrane was estimated to be of 1800 molecules/μm^2 with active Syntaxin 1 molecules concentrating in small domains (of 50-60 nm) where their surface density can be as high as 31,600 molecules/μm^2 [2]. In the context of liposomes (assuming 0.65 nm^2 per lipid), this would correspond to a lipid-to-VAMP2 ratio of 120 and a lipid-to-Syntaxin 1 ratio between 50 and 800. We have previously shown that efficient *in vitro* SNARE-mediated liposome fusion (>5% after 80 min of reaction) requires that both v- and t-SNARE proteins have surface densities of at least 1 protein for 300 lipids [3]. Similar protein-to-lipid ratio was required for efficient Atlastin-mediated liposome fusion *in vitro* [4,5]. By using liposomes with a lipid composition mimicking that of the ER, less Sey 1p (the yeast homolog of Atlastin) was required and fusion was efficient at a lipid-to-protein ratio of 1000 [6]. The SNARE and Atlastin surface densities required for liposome fusion are thus comparable with those allowing fusion mediated by HR1 in our system. How does it compare with the physiological concentration of Mitofusins? To answer this question, we have purified mitochondria from wild-type MEFs and quantified by Western Blot their Mitofusin content by comparison with several concentrations of recombinant MBP-Mfn1 and MBP-Mfn2. By this approach, we measured ~0.22 ng of Mfn1 and ~0.74 ng of Mfn2 per µg of mitochondria (Fig. S5C). By modelling mitochondria as ellipsoids of 1 µm × 1 µm × 10 µm with a density of 1.19 g/cm^3 [7], this leads to 798 Mfn1/μm^2 and 2602 Mfn2/μm^2. In the context of liposomes, this would correspond to lipid-to-protein ratios of 1927 and 591, respectively, and thus to a total lipid-to-Mitofusin ratio of 452. The total concentration of Mitofusin is thus comparable to the lipid-to-protein ratio required for fusion in our *in vitro* system, but the Mfn1 concentration is slightly lower. *In vivo*, Mfn1 could locally concentrate at sites of mitochondrial fusion as suggested by the recent cryo-EM work of the Cohen lab, which showed that mitochondrial fusion occurred at the edge of a docking ring containing high protein densities [8].

Figure S1

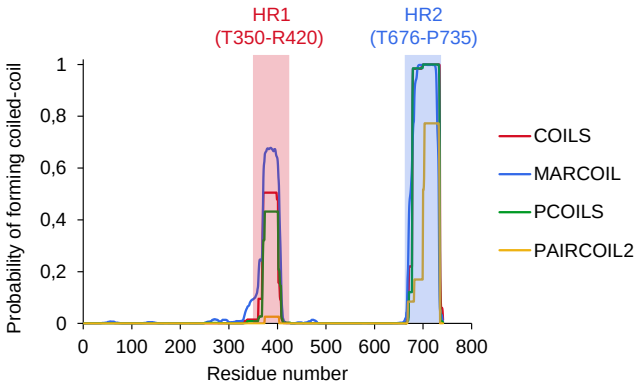

Fig. S1. Coiled-coil forming probabilities for the HR1 and HR2 domains of Mfn1 calculated with various prediction programs: COILS [9], MARCOIL [10], PCOILS [11] and PAIRCOIL2 [12]. All programs predicted that HR2 has a very high probability of forming a coiled-coil structure but they gave lower and divergent probability results for HR1.

Figure S2

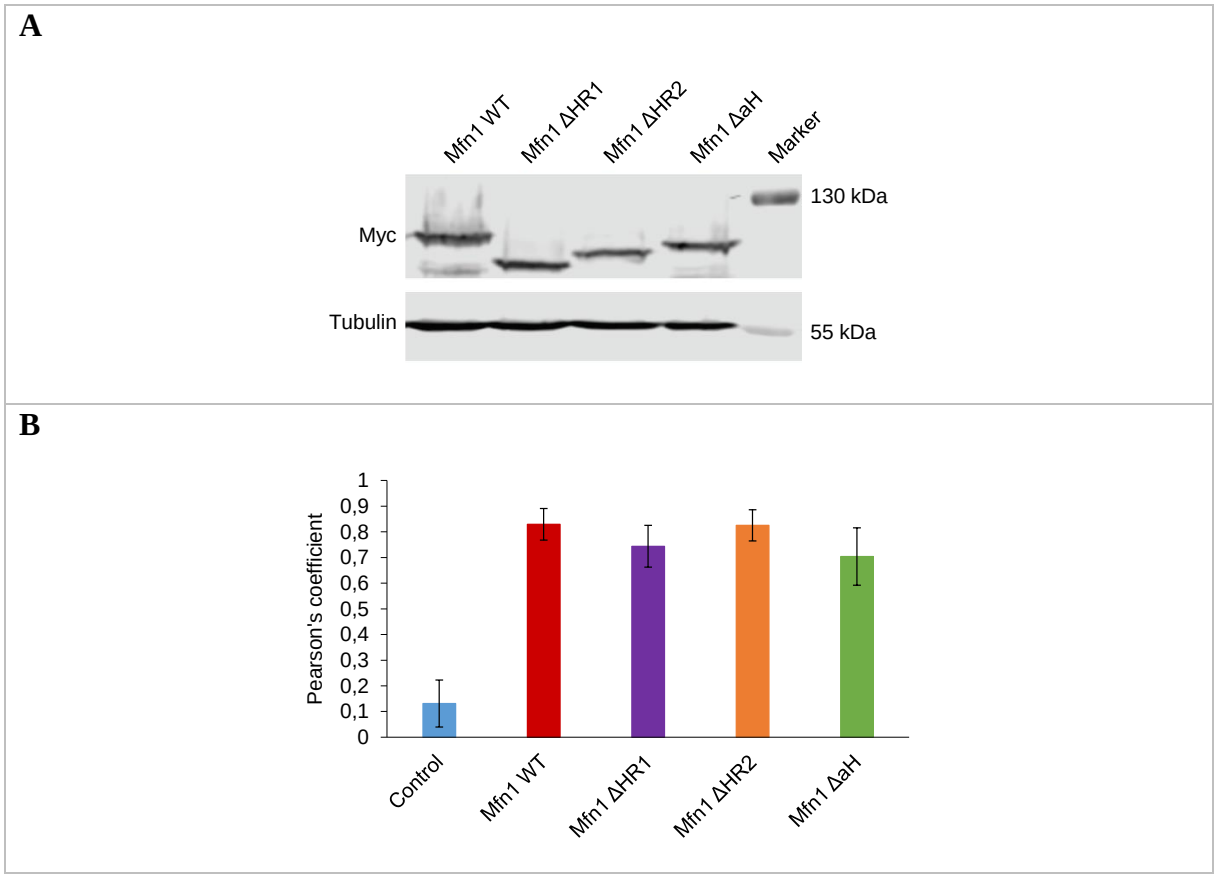

Fig. S2. (A) Expression level of the various Mfn1 variants after transfection in Mfn 1 KO MEFs. Mfn1 constructs were visualized by Western Blot using an antibody directed against their C-terminal Myc tag. All Mfn1 variants were expressed at similar levels when compared with tubulin, although the expression levels appeared slightly higher for wild-type Mfn1 than for heptad repeat or amphipathic helix deleted mutants (representative Western Blot of n=3 independent experiments). (B) Mitochondrial targeting of the various Mfn1 variants determined by analyzing their co-localization with an EGFP molecule targeted to the mitochondrial matrix (Fig. 1). These co-localization experiments (quantified by the Pearson's correlation coefficient, PCC, using the software SlideBook) showed that the PCC of images of Mfn1 variants and mitochondrial EGFP had values larger than 0.7, proving that all Mfn1 variants were efficiently targeted to mitochondria (~25-45 cells for each Mfn1 variant; n=3 independent experiments). Interestingly, both the HR1 deleted mutant and the amphipathic helix deleted mutant displayed slightly lower PCC values (0.74 and 0.70, respectively) compared to the wild-type Mfn1 and the HR2 deleted mutant (0.83 for both variants). It is thus possible that the amphipathic helix of HR1, in addition to its role in mitochondrial fusion, has also a function in mitochondrial

targeting as recently shown for an amphipathic helix located between the transmembrane domain and the HR2 domain of Mfn1 [13].

Figure S3

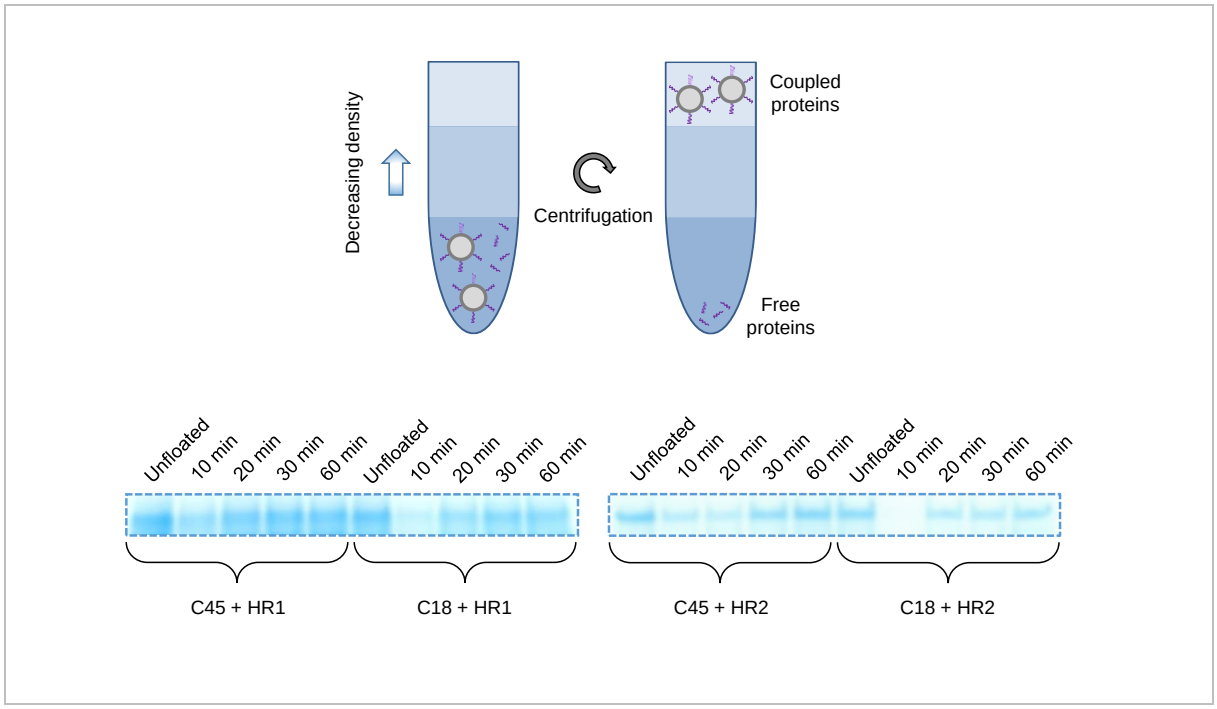

Fig. S3. Kinetics of HR1 and HR2 coupling to maleimide-containing liposomes. The HR1 or HR2 domains of Mfn1 (12.5 µM) were incubated with POPC:C45-or-C18(95:5) liposomes (500 µM of lipids) at 37°C for the indicated time periods, and the reaction mixes were floated-up on a discontinuous nycodenz gradient [14] to separate proteoliposomes from unbound proteins (top panel). The gels (4-12% Bis-Tris Protein Gels from Invitrogen) show that 70-80% of the heptad repeat domains of Mfn1 are coupled to maleimide lipids after 20 min of incubation at 37°C (bottom panel).

Figure S4

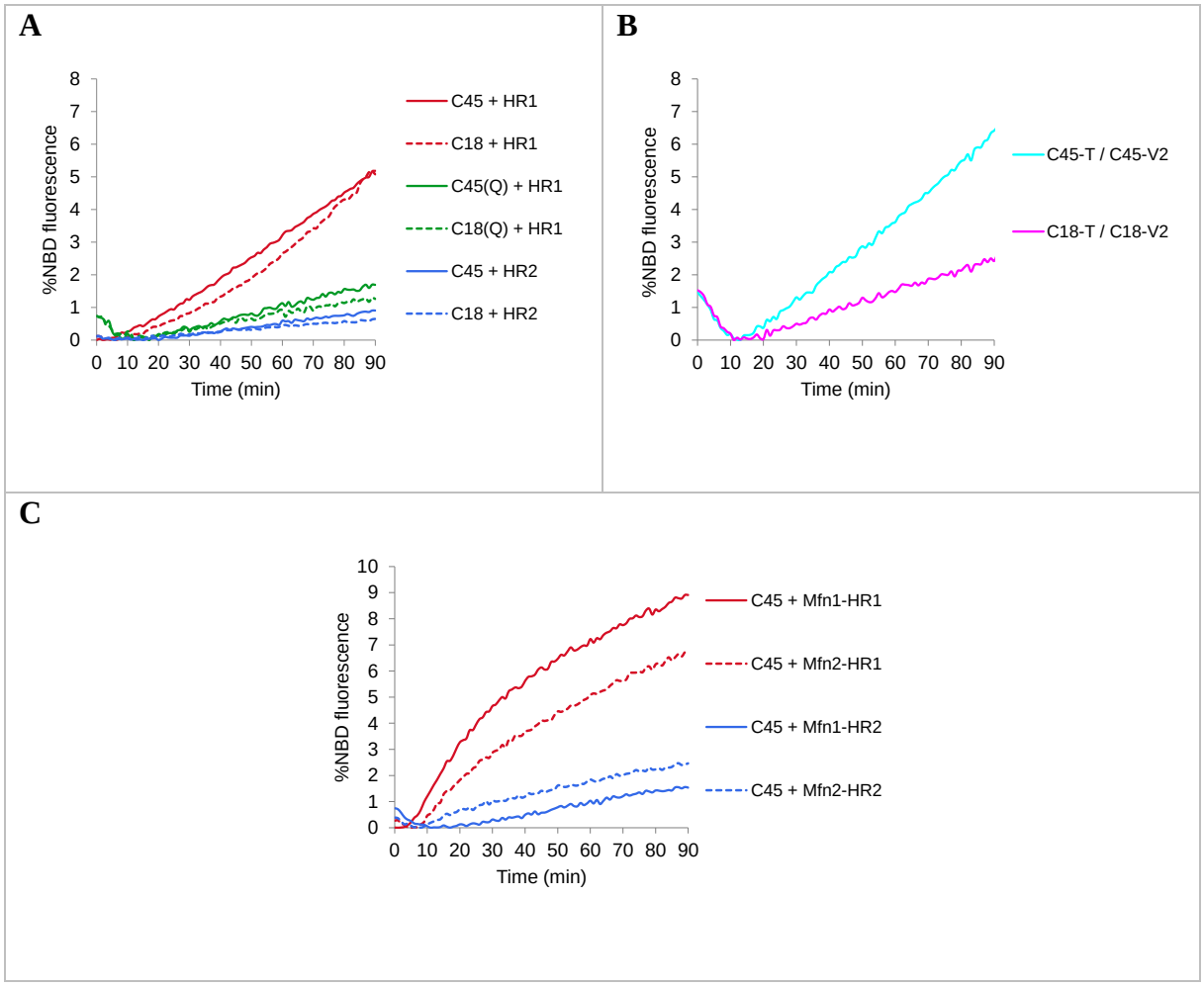

Fig. S4. (A) FRET-based lipid mixing assay between POPC:C45-or-C18(95:5) and POPC:C45-or-C18:DOPE-NBD:DOPE-Rho(92:5:1.5:1.5) liposomes (500 µM of lipids) following the addition at t=0 of recombinant heptad repeat domains of Mfn1 (12.5 µM) in the absence or presence of 1 mM dithiothreitol (DTT) in order to quench maleimide lipids (Q). Recombinant proteins displayed slightly variable and usually lower fusion activity compared to synthetic peptides (see fusion data of Fig. 2B). (B) Lipid mixing between pre-formed proteoliposomes consisting of the cytosolic domain of the t-SNARE Syn1A/SNAP25 (T) anchored to POPC:C45-or-C18(95:5) membranes and pre-formed proteoliposomes consisting of the cytosolic domain of the v-SNARE VAMP2 (V2) anchored to POPC:C45-or-C18:DOPE-NBD:DOPE-Rho(92:5:1.5:1.5) membranes. (C) FRET-based lipid mixing assay between POPC:C45(95:5) and POPC:C45:DOPE-NBD:DOPE-Rho(92:5:1.5:1.5) liposomes (500 µM of lipids) in the presence of synthetic heptad repeat domains of Mfn1 or Mfn2 (12.5 µM) added at t=0.

Figure S5

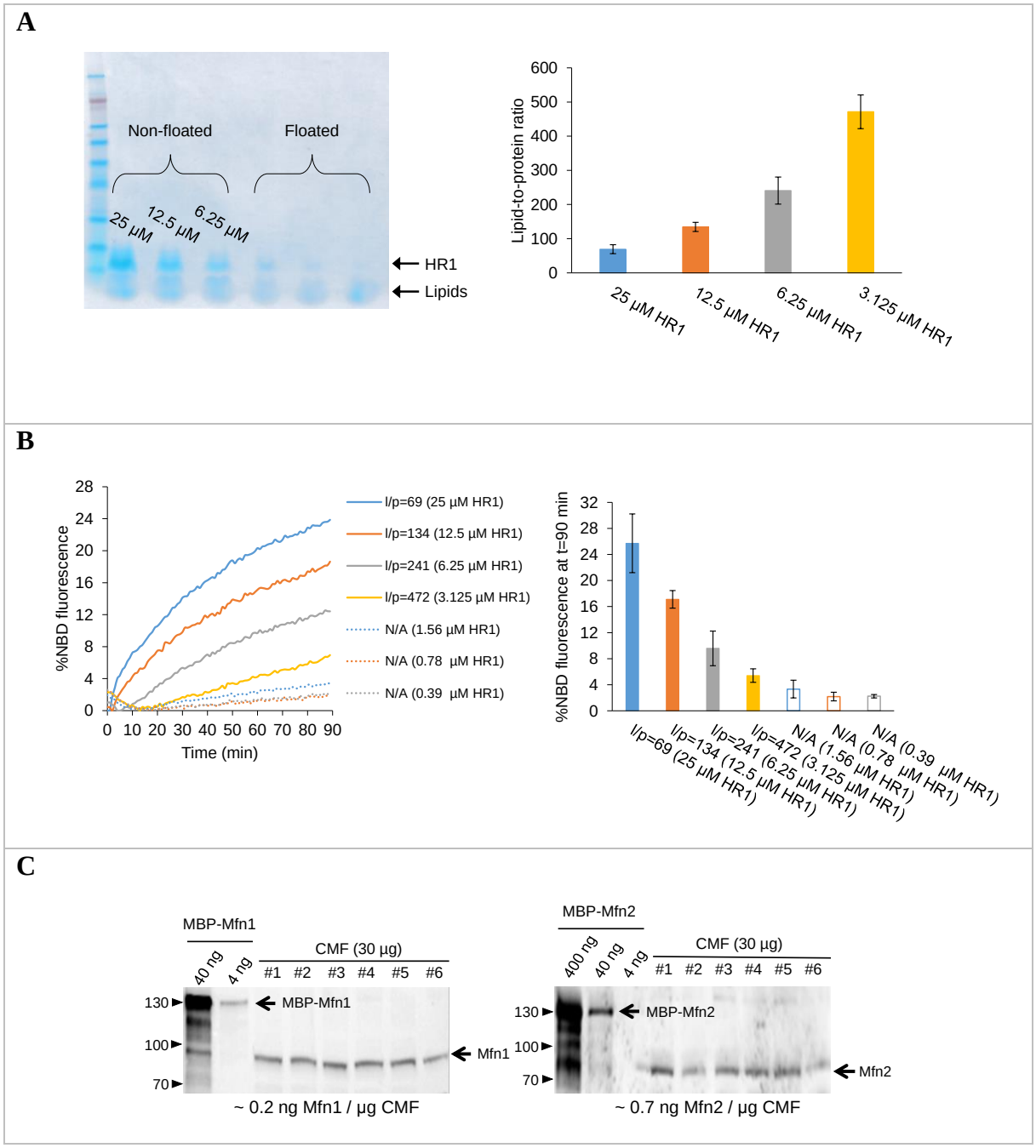

Fig. S5. (A) Determination of the lipid-to-protein ratio in POPC:C18(95:5) liposomes after incubation with different concentrations of HR1. Liposomes (500 µM of lipids) were incubated with HR1 (from 25 µM down to 0.39 µM) for 1 hour at 37°C, and the reaction mixes were floated-up on a discontinuous nycodenz gradient [14] to separate proteoliposomes from uncoupled proteins. Protein and lipid recoveries in the floated samples were estimated by SDS-PAGE stained with Coomassie (4-12% Bis-Tris Protein Gels from Invitrogen) upon comparison with the non-floated samples. Silver staining was used when the peptide could not be clearly

detected by Coomassie. The protein concentration in the floated proteoliposomes resulting from incubation with HR1 at 1.56 µM or less could not be measured (detection limit of silver staining for this peptide). The left panel shows one representative gel, and the right panel the actual lipid-to-HR1 ratios in the proteoliposomes after incubation with a decreasing concentration of HR1 (n=3 independent experiments; error bars are standard deviations). (B) Liposome fusion activity as a function of the surface density of HR1 on the liposome membrane. Different concentrations of HR1 were added at t=0 of the FRET assay (from 25 µM down to 0.39 µM for 500 µM of lipids). Significant lipid mixing (larger than 5% after 90 min of reaction) requires an HR1 surface density of at least 1 protein for 470 lipids (obtained by the addition of 3.125 µM HR1 at the beginning of the fusion assay). Of note, addition of 12.5 µM of HR1, as performed throughout the manuscript, leads to a lipid-to-HR1 ratio of 130. The left panel shows one representative set of titration experiments, and the right panel the average extent of lipid mixing after 90 min of reaction (n=3 independent experiments; error bars are standard deviations). (C) Estimation of the Mfn1 and Mfn2 content in MEFs. Crude mitochondrial fractions (CMF, n=6 independent isolations) of MEFs were isolated by differential centrifugation as described [15]. Human Mfn1 and Mfn2 appended with an N-terminal Maltose Binding Protein (MBP) tag [16] were expressed and purified as described for HR1 and HR2 domains. The indicated protein amounts were separated by SDS-PAGE, transferred to nitrocellulose membranes and decorated with rabbit polyclonal antibodies specific for Mfn1 [17] or Mfn2 [18]. Chemiluminescent signal of secondary antibodies was recorded with a CCD camera (Syngene G-box) and quantitatively analyzed with ImageJ. The amount of Mfn1 and Mfn2 in 30 µg of CMF was estimated from the amount of purified MBP-Mfn1 and MBP-Mfn2 co-decorated on the same membrane: 0.22 +/- 0.04 ng Mfn1/µg CMF and 0.74 +/- 0.22 ng Mfn2/µg CMF.

Figure S6

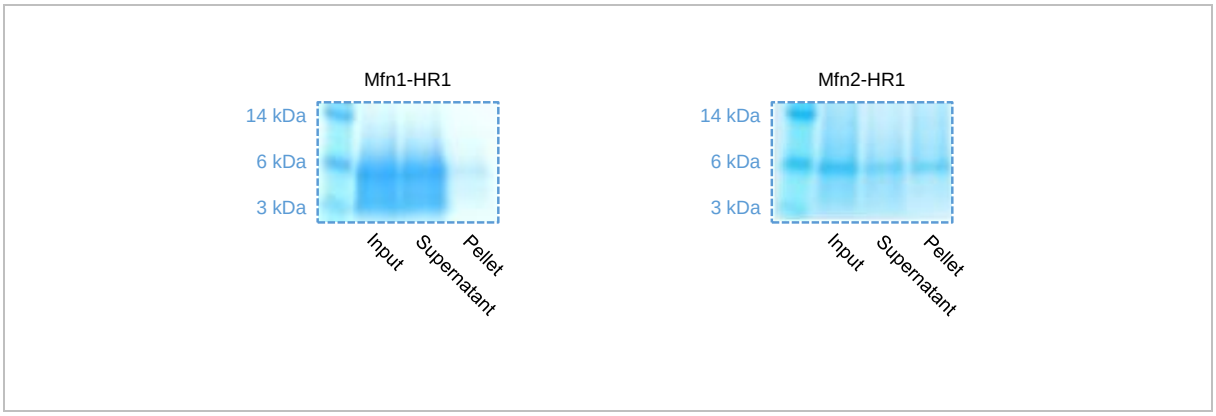

Fig. S6. Aggregation properties of the HR1 domain of Mfn1 or Mfn2. HR1 domains were centrifuged for 45 min at 200,000 g in a TLA 120.2 rotor (Beckman). The resulting supernatants and pellets were isolated in the same final volume and applied to a gel (4-12% Bis-Tris Protein Gel from Invitrogen) for analysis and comparison with the initial protein material (input). In the case of the HR1 domain of Mfn1, more than 90% is recovered in the supernatant fraction, whereas the HR1 domain of Mfn2 has a larger tendency to aggregate with more than 50% of the protein found in the pellet fraction.

Figure S7

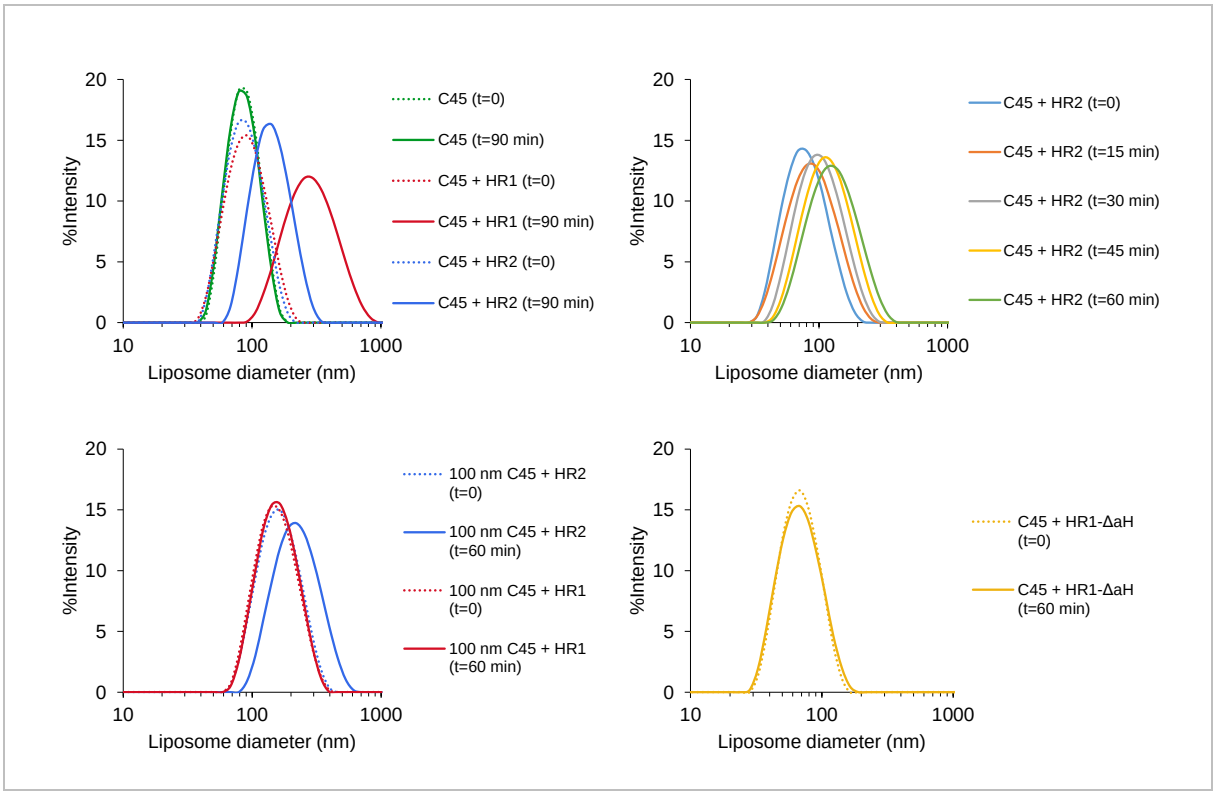

Fig. S7. Liposome-liposome docking by the heptad repeat domains of Mfn1 probed by Dynamic Light Scattering (DLS). Top left, the size (diameter) of POPC:C45:DOPE-NBD:DOPE-Rho(92:5:1.5:1.5) liposomes prepared by extrusion was measured by DLS before and after 90 min of incubation at 37°C with the HR1 or HR2 domain of Mfn1 (12.5 µM of proteins and 500 µM of lipids in the reaction mix; samples were diluted 5 times right before DLS measurement). Both the HR1 and HR2 domains induce an increase of particle size (as a result of liposome docking and/or fusion). Liposomes are overall larger after incubation with HR1 (than after incubation with HR2), which could be explained by the presence of liposome clusters containing larger (fused) liposomes (resulting from the fusion of a subpopulation of small highly curved liposomes) in the presence of HR1 (see also the electron microscopy pictures of Fig. 4B). Top right, kinetics of POPC:C45(95:5) liposomes docking by HR2 monitored under the same experimental conditions as in the FRET-based lipid mixing assay (500 µM of lipids and 12.5 µM of proteins incubated together at 37°C). The liposome size distribution started shifting toward larger values (due to docking since no HR2-mediated liposome fusion was measured in the FRET assay) after 10-15 min, and the liposome size increased continuously during the reaction. Bottom left, size distribution of 100 nm POPC:C45(95:5) liposomes prepared by extrusion before and after 1 hour of incubation at 37°C

with HR1 or HR2 (500 μM of lipids and 12.5 μM of proteins). No liposome size shift was observed with HR1, whereas HR2 could still dock these larger liposomes. Bottom right, size distribution of POPC:C45(95:5) liposomes before and after 1 hour of incubation at 37°C with the amphipathic helix deleted HR1 mutant, HR1-ΔaH (500 μM of lipids and 12.5 μM of proteins). No liposome size shift was observed with this mutant, indicating that it cannot mediate liposome docking.

Figure S8

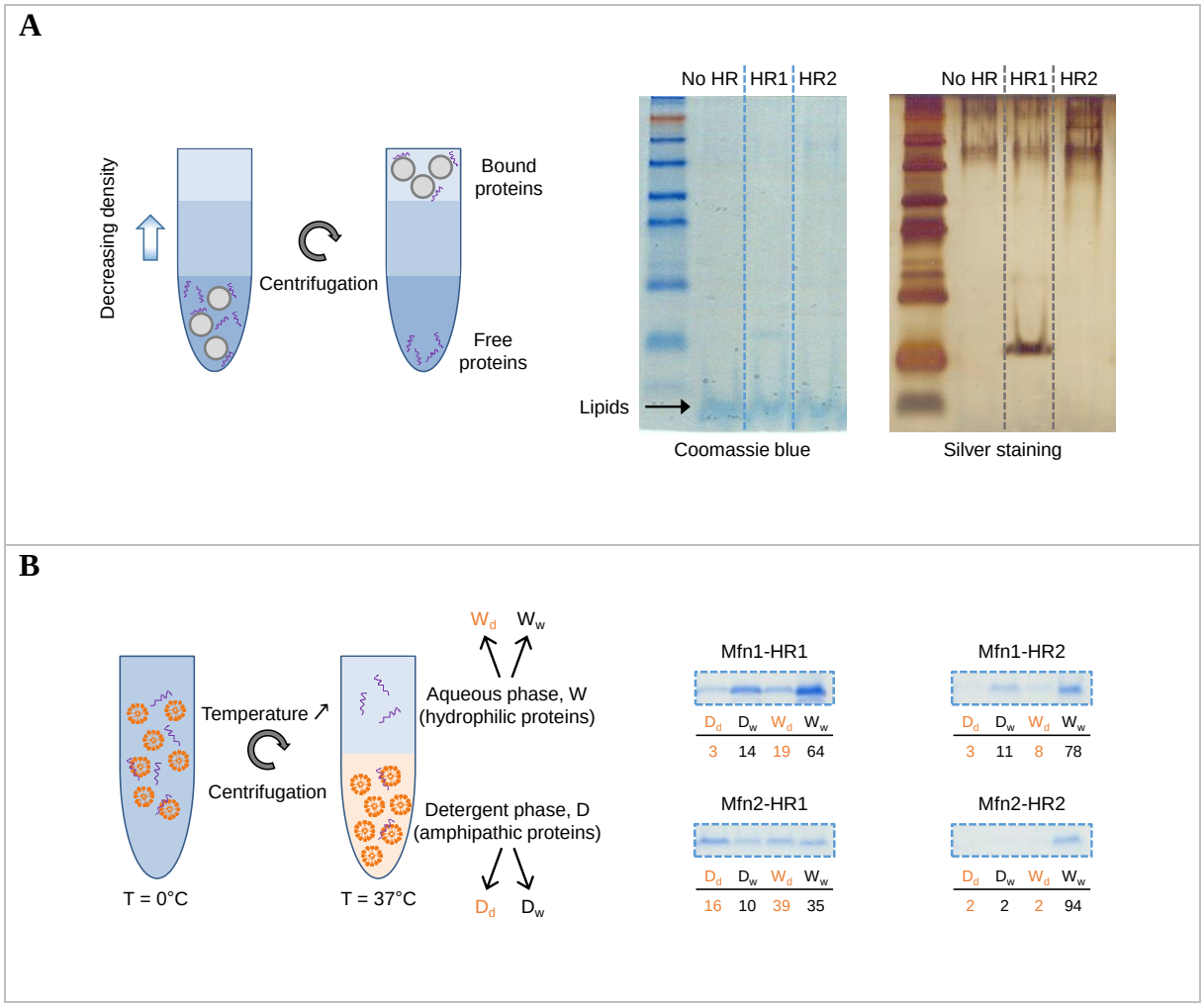

Fig. S8. (A) Interaction between recombinant heptad repeat domains of Mfn1 and protein-free liposomes analyzed by a liposome co-floatation assay. POPC liposomes (500 µM of lipids) were incubated for 30 min at 37°C with the HR1 or HR2 domain of Mfn1 (12.5 µM), and protein-bound liposomes were isolated on a nycodenz floatation gradient [14]. Membrane binding by HR1 could be revealed by silver staining. (B) Phase separation of recombinant heptad repeat domains of Mfn1 or Mfn2 in solutions of Triton X-114 [19]. Heptad repeat domains (2.5 µM) were incubated for 15 min at 37°C in a solution of 0.5% Triton X-114 and centrifuged to separate the detergent phase (D) from the aqueous phase (W). Each phase was then subjected to a second round of extraction and separated as two sub-phases (D_d, D_w and W_d, W_w). The amount of protein in the detergent (respectively aqueous) phase was calculated as the sum of the two detergent (respectively aqueous) sub-phases content. HR1 domains were partially found in the detergent phase (22-55%), whereas HR2 domains were mainly recovered in the aqueous phase (89-96%).

Figure S9

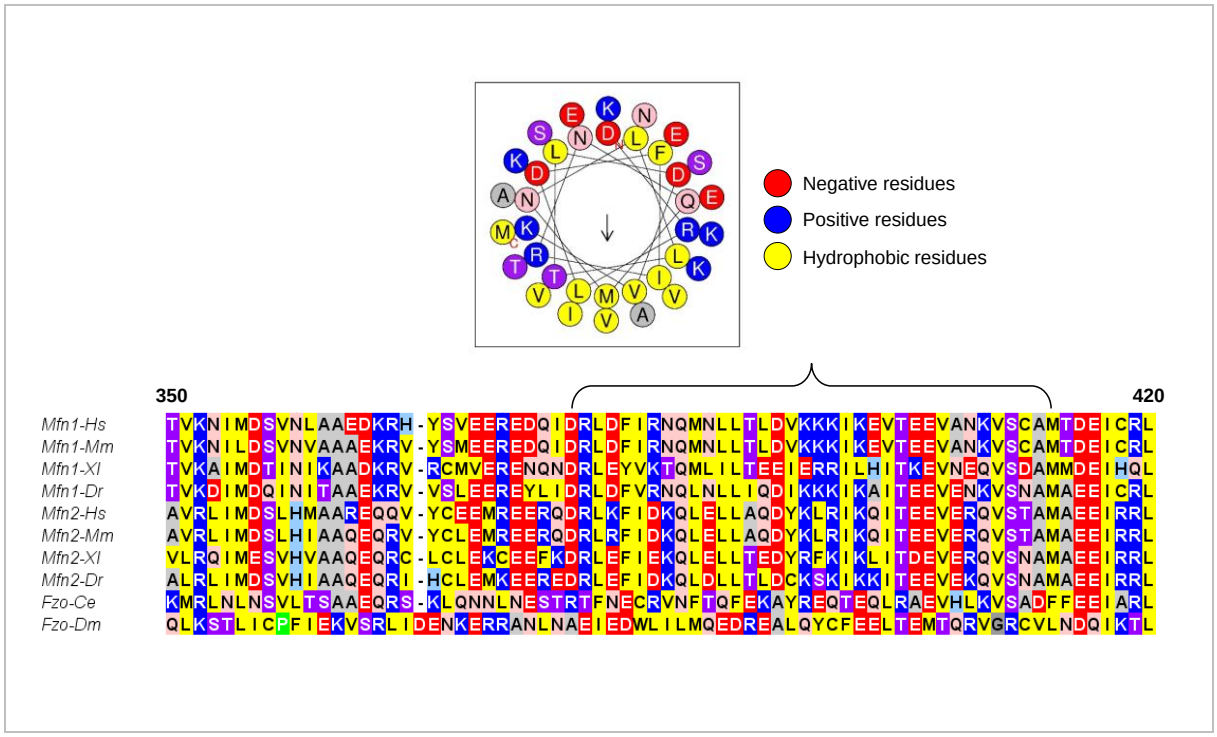

Fig. S9. Top, helical wheel representation of HR1 in the region (378-413) generated by HeliQuest. Bottom, alignment of the HR1 domains from several Mitofusine-like proteins, showing that the hydrophobic and charged residues of the amphipathic helix are well conserved across species. Hs, Homo sapiens; Mm, Mus musculus; Xl, Xenopus laevis; Dr, Danio rerio; Ce, Caenorhabditis elegans; Dm, Drosophila melanogaster. Residue numbers are from human Mfn1.

Figure S10

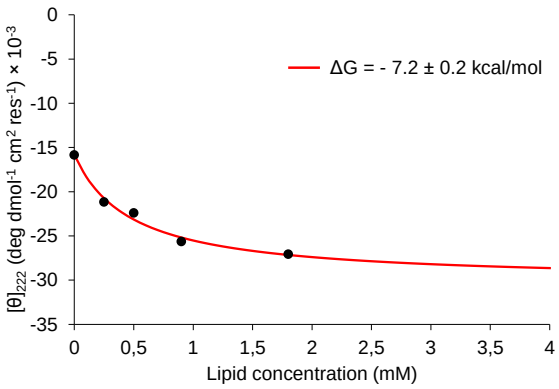

Fig. S10. Circular dichroism spectra of the HR1 domain of Mfn1 were recorded after 30 min of incubation at 37°C with POPC:C45(95:5) liposomes using various lipid-to-protein molar ratios (12.5 µM of proteins and 1.8, 0.9, 0.5 and 0.25 mM of lipids). The absolute value of the mean residue molar ellipticity of HR1 at 222 nm increases when the lipid/protein molar ratio increases, indicating that the amphipathic helix of HR1 becomes more structured upon interaction with lipid bilayers. This increase of HR1 helicity with liposomes concentration was used to deduce the free energy of HR1 partitioning-folding into the liposome membrane (see methods section for details): $\Delta G = - 7.2 \pm 0.2$ kcal/mol.

Figure S11

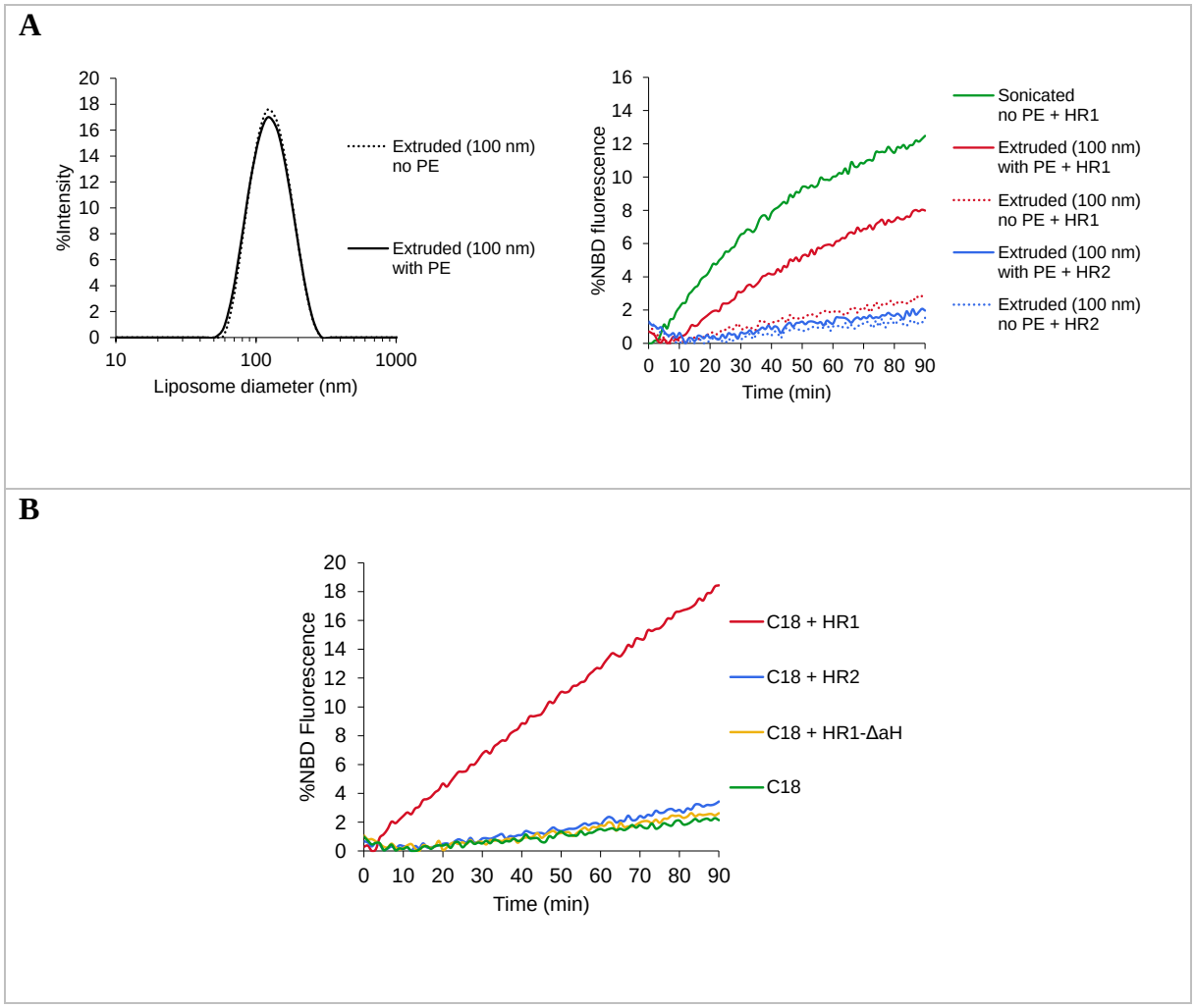

Fig. S11. (A) Left, Dynamic Light Scattering on 100 nm POPC or POPC:DOPE (70:30) liposomes made by extrusion. The presence of 30 mol% PE in the liposome membrane has no effect on the liposomes size. Right, FRET-based lipid mixing assay between maleimide-containing fluorescent/donor liposomes and maleimide-free non-fluorescent/acceptor liposomes (500 µM of lipids) containing or not 30 mol% PE lipids (asymmetrical liposome fusion system illustrated on Fig. 5, top middle panel) after addition of the HR1 domain of Mfn1 (12.5 µM) at t=0. Liposomes were generated either by sonication or extrusion using a polycarbonate membrane with a 100 nm pore size. In this asymmetrical configuration, HR1 could still mediate the fusion of sonicated liposomes with the same efficiency as liposomes formed by the standard method (Fig. 5, purple curve) but was unable to fuse 100 nm liposomes. Fusion between 100 nm liposomes was partially restored when acceptor liposomes contained 30 mol% PE lipids. HR2 did not present any fusogenic activity even when 30 mol% PE was included in the acceptor liposomes. (B) FRET-based lipid mixing experiments between

POPC:C18:DOPE-NBD:DOPE-Rho(92:5:1.5:1.5) and POPC:C18(95:5) liposomes incubated at t=0 of the assay with HR1, HR2 or the amphipathic helix deleted HR1 mutant, HR1-ΔaH (500 µM of lipids and 12.5 µM of proteins). No significant lipid mixing was measured with the HR1-ΔaH mutant, confirming the importance of the amphipathic helix of HR1 in membrane fusion.

Figure S12

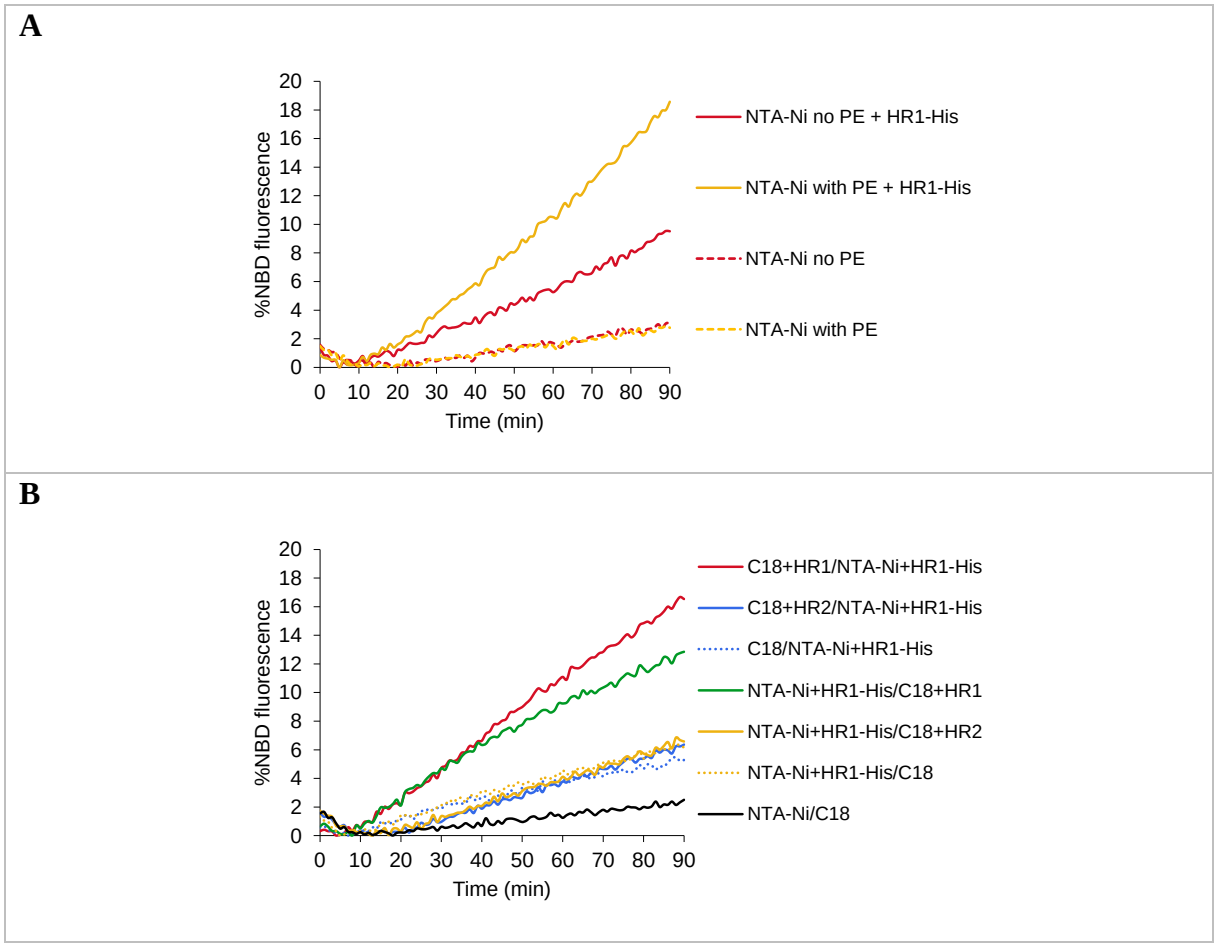

Fig. S12. Liposome fusion experiments using the NTA-Ni anchoring strategy. (A) FRET-based lipid mixing experiments between POPC:DOGS-NTA-Ni:DOPE-NBD:DOPE-Rho(92:5:1.5:1.5) and POPC:DOGS-NTA-Ni(95:5) liposomes in the absence or presence of HR1 with a C-terminal His_6 tag added at t=0 of the assay (500 µM of lipids and 12.5 µM of proteins). The HR1-His_6 fragment induced efficient lipid mixing between liposomes and fusion was strongly activated when the liposome membrane contained 30 mol% DOPE lipids (at the expense of POPC lipids). (B) FRET-based lipid mixing experiments between non-fluorescent maleimide-containing liposomes and fluorescent NTA-Ni-containing liposomes or between non-fluorescent NTA-Ni-containing liposomes and fluorescent maleimide-containing liposomes, incubated at t=0 of the assay with HR1 and HR1-His_6, HR2 and HR1-His_6 or HR1-His_6 alone to investigate the potential role of HR1/HR2 interaction in fusion (500 µM of lipids and 12.5 µM of proteins). Similar fusion extents were measured between HR1 liposomes and protein-free or HR2 liposomes, indicating that the fusion activity observed in the HR1/HR2 systems was due to HR1 interacting with the liposome membrane and not with HR2.

References

1. Takamori S, Holt M, Stenius K, Lemke EA, Grønborg M, Riedel D, Urlaub H, Schenck S, Brügger B, Ringler P, et al. (2006) Molecular anatomy of a trafficking organelle. *Cell* **127**: 831–846.

2. Sieber JJ, Willig KI, Kutzner C, Gerding-Reimers C, Harke B, Donnert G, Rammner B, Eggeling C, Hell SW, Grubmüller H, et al. (2007) Anatomy and dynamics of a supramolecular membrane protein cluster. *Science* **317**: 1072–1076.

3. Ji H, Coleman J, Yang R, Melia TJ, Rothman JE, Tareste D (2010) Protein determinants of SNARE-mediated lipid mixing. *Biophys J* **99**: 553–560.

4. Orso G, Pendin D, Liu S, Tosetto J, Moss TJ, Faust JE, Micaroni M, Egorova A, Martinuzzi A, McNew JA, et al. (2009) Homotypic fusion of ER membranes requires the dynamin-like GTPase atlastin. *Nature* **460**: 978–983.

5. Anwar K, Klemm RW, Condon A, Severin KN, Zhang M, Ghirlando R, Hu J, Rapoport TA, Prinz WA (2012) The dynamin-like GTPase Sey1p mediates homotypic ER fusion in S. cerevisiae. *J Cell Biol* **197**: 209–217.

6. Lee M, Ko YJ, Moon Y, Han M, Kim HW, Lee SH, Kang K, Jun Y (2015) SNAREs support atlastin-mediated homotypic ER fusion in Saccharomyces cerevisiae. *J Cell Biol* **210**: 451–470.

7. Graham JM, Rickwood D (1997) *Subcellular Fractionation: A Practical Approach*. Oxford University Press.

8. Brandt T, Cavellini L, Kühlbrandt W, Cohen MM (2016) A mitofusin-dependent docking ring complex triggers mitochondrial fusion in vitro. *elife* **5**:

9. Lupas A, Van Dyke M, Stock J (1991) Predicting coiled coils from protein sequences. *Science* **252**: 1162–1164.

10. Delorenzi M, Speed T (2002) An HMM model for coiled-coil domains and a comparison with PSSM-based predictions. *Bioinformatics* **18**: 617–625.

11. Lupas A (1996) Prediction and analysis of coiled-coil structures. *Meth Enzymol* **266**: 513–525.

12. McDonnell AV, Jiang T, Keating AE, Berger B (2006) Paircoil2: improved prediction of coiled coils from sequence. *Bioinformatics* **22**: 356–358.

13. Huang X, Zhou X, Hu X, Joshi AS, Guo X, Zhu Y, Chen Q, Prinz WA, Hu J (2017) Sequences flanking the transmembrane segments facilitate mitochondrial localization and membrane fusion by mitofusin. *Proc Natl Acad Sci U S A* **114**: E9863–E9872.

14. Scott BL, Van Komen JS, Liu S, Weber T, Melia TJ, McNew JA (2003) Liposome fusion assay to monitor intracellular membrane fusion machines. *Meth Enzymol* **372**: 274–300.

15. Malka F, Auré K, Goffart S, Spelbrink JN, Rojo M (2007) The mitochondria of cultured mammalian cells: I. Analysis by immunofluorescence microscopy, histochemistry, subcellular fractionation, and cell fusion. *Methods Mol Biol* **372**: 3–16.

16. Cabrita LD, Dai W, Bottomley SP (2006) A family of E. coli expression vectors for laboratory scale and high throughput soluble protein production. *BMC Biotechnol* **6**: 12.

17. Yoon YS, Yoon DS, Lim IK, Yoon SH, Chung HY, Rojo M, Malka F, Jou MJ, Martinou JC, Yoon G (2006) Formation of elongated giant mitochondria in DFO-induced cellular senescence: involvement of enhanced fusion process through modulation of Fis1. *J Cell Physiol* **209**: 468–480.

18. Rojo M, Legros F, Chateau D, Lombès A (2002) Membrane topology and mitochondrial targeting of mitofusins, ubiquitous mammalian homologs of the transmembrane GTPase Fzo. *J Cell Sci* **115**: 1663–1674.

19. Bordier C (1981) Phase separation of integral membrane proteins in Triton X-114 solution. *J Biol Chem* **256**: 1604–1607.